

# WISE J080822.18–644357.3 – a 45 Myr-old accreting M dwarf hosting a primordial disc

Simon J. Murphy<sup>★1</sup>, Eric E. Mamajek<sup>2,3</sup> and Cameron P. M. Bell<sup>4</sup>

<sup>1</sup>*School of Physical, Environmental and Mathematical Sciences, University of New South Wales Canberra, ACT 2600, Australia*

<sup>2</sup>*Jet Propulsion Laboratory, California Institute of Technology, 4800 Oak Grove Dr., Pasadena, CA 91109, USA*

<sup>3</sup>*Department of Physics & Astronomy, University of Rochester, Rochester, NY 14627, USA*

<sup>4</sup>*Leibniz Institute for Astrophysics Potsdam (AIP), An der Sternwarte 16, 14482 Potsdam, Germany*

Accepted 2018 February 16. Received 2018 February 13; in original form 2017 March 10

## ABSTRACT

WISE J080822.18–644357.3 (WISE J0808–6443) was recently identified as a new M dwarf debris disc system and a candidate member of the 45 Myr-old Carina association. Given that the strength of its infrared excess ( $L_{\text{IR}}/L_{\star} \approx 0.1$ ) appears to be more consistent with a young protoplanetary disc, we present the first optical spectra of the star and reassess its evolutionary and membership status. We find WISE J0808–6443 to be a Li-rich M5 star with strong H $\alpha$  emission ( $-125 < \text{EW} < -65 \text{ \AA}$  over 4 epochs) whose strength and broad width are consistent with accretion at a low level ( $\sim 10^{-10} M_{\odot} \text{ yr}^{-1}$ ) from its disc. The spectral energy distribution of the star is consistent with a primordial disc and is well-fit using a two-temperature black-body model with  $T_{\text{inner}} \approx 1100 \text{ K}$  and  $T_{\text{outer}} \approx 240 \text{ K}$ . AllWISE multi-epoch photometry shows the system exhibits significant variability in the 3.4  $\mu\text{m}$  and 4.6  $\mu\text{m}$  bands. We calculate an improved proper motion based on archival astrometry, and combined with a new radial velocity, the kinematics of the star are consistent with membership in Carina at a kinematic distance of  $90 \pm 9 \text{ pc}$ . The spectroscopic and photometric data are consistent with WISE J0808–6443 being a  $\sim 0.1 M_{\odot}$  Classical T-Tauri star and one of the oldest known accreting M-type stars. These results provide further evidence that the upper limit on the lifetimes of gas-rich discs – and hence the timescales to form and evolve protoplanetary systems – around the lowest mass stars may be longer than previously recognised, or some mechanism may be responsible for regenerating short-lived discs at later stages of pre-main sequence evolution.

**Key words:** stars: kinematics and dynamics – stars: pre-main-sequence – stars: fundamental parameters – solar neighbourhood – open clusters and associations: individual: Carina

## 1 INTRODUCTION

Dust and gas-rich discs around pre-main sequence (pre-MS) stars are an inevitable consequence of angular momentum conservation during the star formation process (Shu, Adams & Lizano 1987; McKee & Ostriker 2007). Discs have been observed around young stars of all masses and can exhibit a variety of morphologies depending on the myriad external factors (for example, host star mass, multiplicity, dynamical history, proximity to massive stars) and internal processes (accretion, grain coagulation/processing, photo-evaporation, gravitational settling, planet formation) at work throughout their evolution (Williams & Cieza 2011, and references therein).

The most important parameter in understanding disc evolution is the disc lifetime. Firstly, as it reflects the dominant physical processes driving dissipation of the disc but also because it sets an upper limit on the timescale of giant planet formation. Observationally, the frequency of discs around pre-MS stars rapidly declines with time. Primordial (i.e. first generation) discs supporting ongoing accretion of gas onto the star are common at ages of 1–2 Myr in regions like Orion and Taurus-Auriga, but by 10–15 Myr they

appear to be very rare (Haisch, Lada & Lada 2001; Hillenbrand 2005; Sicilia-Aguilar et al. 2005; Hernández et al. 2007a; Mamajek 2009). Near and mid-infrared disc fractions in young clusters and star-forming regions are consistent with median primordial disc lifetimes of 4–5 Myr (Bell et al. 2013; Pecauc & Mamajek 2016), with a similar or slightly shorter lifetime inferred for circumstellar accretion (Fedele et al. 2010). Variations in disc frequency between supposedly coeval groups can be explained by a variety of factors. For instance, shorter disc lifetimes have been proposed for stars in multiple systems (e.g. Bouwman et al. 2006), those in the vicinity of massive stars (Guarcello et al. 2016; Balog et al. 2007; Johnstone, Hollenbach & Bally 1998) and in dense stellar environments (e.g. Pfalzner, Umbreit & Henning 2005; Luhman et al. 2008; Thies et al. 2010; Olczak et al. 2012). Conversely, there are several notable examples of gas-rich discs and accretion at ages greater than  $\sim 10 \text{ Myr}$ . These include the T Tauri star MP Mus (PDS 66) in the 10–20 Myr-old Lower-Cen-Cru subgroup of Sco-Cen (Mamajek, Meyer & Liebert 2002; but see membership discussion in Murphy, Lawson & Bessell 2013) and a handful of other Sco-Cen accretors (Murphy & Lawson 2015; Pecauc & Mamajek 2016), the lithium-poor M3+M3 binary St 34 in Taurus (White & Hillenbrand 2005) and the A-type stars 49 Ceti ( $\sim 40 \text{ Myr}$ ; Zuckerman & Song 2012) and HD 21997 ( $\sim 30 \text{ Myr}$ ; Moór et al. 2011). Long-lived accretion has also been observed outside the immediate solar neighbourhood,

<sup>★</sup> E-mail: s.murphy@adfa.edu.au

including in the  $\sim 13$  Myr-old double cluster  $\eta$  and  $\chi$  Persei (Currie et al. 2007a,b), NGC 6611 (De Marchi et al. 2013a), NGC 3603 (Beccari et al. 2010) and the Magellanic Clouds (Spezzi et al. 2012; De Marchi, Beccari & Panagia 2013b).

Unsurprisingly, stellar mass plays a major role in driving disc evolution. Early *Spitzer Space Telescope* surveys of nearby young clusters (e.g. Lada et al. 2006; Carpenter et al. 2006; Hernández et al. 2007a,b; Kennedy & Kenyon 2009) strongly suggested primordial discs around low-mass stars can persist longer than solar and higher-mass stars. For example, in their census of discs across the  $\sim 11$  Myr (Pecaut, Mamajek & Bubar 2012) Upper Sco subgroup of Sco-Cen, Luhman & Mamajek (2012) (also see Carpenter et al. 2006, 2009; Chen et al. 2011) found 10 per cent of members of spectral types B–G possessed inner discs, while this reached  $\sim 25$  per cent for M5–L0 stars, indicating that a significant fraction of primordial discs around low-mass stars can survive for at least 10 Myr. These findings were recently generalised by Ribas, Bouy & Merín (2015), who undertook an analysis of over 1,400 spectroscopically-confirmed members of nearby ( $< 500$  pc) associations of ages 1–100 Myr, finding that high-mass ( $> 2 M_{\odot}$  in their study) stars dispersed their disks up to twice as fast as low-mass stars. Together, the results of these studies imply that the mechanisms responsible for removing circumstellar gas and dust operate less efficiently around lower-mass stars and hence longer timescales may be possible for the formation of planetary systems around such hosts.

Clearly, the discovery of additional ‘old’ pre-MS stars hosting primordial discs and showing signs of accretion would be useful in better understanding the evolution and dissipation of discs, especially extreme examples much older than 10 Myr. Through the work of the NASA *Disk Detective* citizen science project<sup>1</sup> (described in Kuchner et al. 2016), Silverberg et al. (2016) recently identified WISE J080822.18–644357.3 (hereafter WISE J0808–6443) as an M dwarf exhibiting significant excess emission in the 12 and 22  $\mu\text{m}$  bands of the *Widefield Infrared Survey Explorer* (WISE) survey (Wright et al. 2010). Adopting the proper motion provided by the Southern Proper Motion Catalog (SPM4; Girard et al. 2011), Silverberg et al. used the Bayesian Analysis for Nearby Young AssociatiONs II tool (BANYAN II; Malo et al. 2013; Gagné et al. 2014) to establish whether the star was associated with any of the seven nearest young moving groups in the Solar neighbourhood (see reviews by Zuckerman & Song 2004; Torres et al. 2008; Mamajek 2016), finding a 93.9 per cent probability that it is a member of the 45 Myr-old Carina association at a distance of  $\sim 65$  pc. Silverberg et al. (2016) classified the star as hosting a second-generation debris disc, whereas the strength of its infrared excess ( $L_{\text{IR}}/L_{\star} \approx 0.1$ ) appears to be more consistent with a young primordial disc (Wyatt 2008). If such a disc is confirmed, WISE J0808–6443 would be one of the oldest known M dwarf protoplanetary disc hosts and a benchmark object through which to study late-stage disc evolution in low-mass stars. Despite the proper motion match to Carina, Silverberg et al. presented no spectroscopic evidence for either youth or group membership. In this work we test their claims by analysing new optical spectra of WISE J0808–6443 (Section 2), deriving a revised proper motion for the star from archival astrometry (Section 3) and reanalysing its spectral energy distribution, infrared excess (Section 4) and isochronal age (Section 5). With this new information we re-evaluate the evolutionary state of the star-disc system and discuss its origins with regards to the dozen or so known young moving groups near the Sun.

## 2 SPECTROSCOPIC OBSERVATIONS

We acquired four spectra of WISE J0808–6443 during 2017 January and February using the Wide Field Spectrograph (WiFeS; Dopita et al. 2007) on the ANU 2.3-m telescope at Siding Spring Observatory. The R7000 grating gives a resolution of  $R \approx 7000$  over a wavelength range of 5250–7000 Å, while the R3000 grating covers 5400–9700 Å at a resolution of  $R \approx 3000$ . Details of the instrument setup and reduction process, including the measurement of radial velocities, are provided in Murphy & Lawson (2015) and Bell, Murphy & Mamajek (2017). The results of these observations are given in Table 1 and the R3000 spectrum is shown in Fig. 1.

WISE J0808–6443 is clearly of mid-M spectral type, with pronounced  $H\alpha$  and He I emission. We also detected strong Li I  $\lambda 6708$  absorption in the R7000 spectra and weak ( $\sim 1$  Å) forbidden [O I]  $\lambda 6300$  emission in all four observations. We measured the equivalent width (EW) of the broad  $H\alpha$  line by direct integration of the line profile. After comparing the R3000 spectrum to the SDSS average M dwarf templates of Bochanski et al. (2007) we estimate a spectral type of approximately M5, in agreement with the  $M4.8 \pm 0.2$  average of the R1, R2, R3, TiO8465, c81 and VO2 molecular indices (covering 7800–8500 Å), as calibrated by Riddick et al. (2007). From the three R7000 spectra we calculate a weighted mean radial velocity of  $22.7 \pm 0.5 \text{ km s}^{-1}$  and  $\text{EW}[\text{Li I}] = 380 \pm 20 \text{ mÅ}$ . Within the limits of the modest WiFeS resolution, the radial velocity appears constant on timescales of  $\sim 1$  month and the star’s cross correlation function is consistent with a slowly-rotating ( $v \sin i \lesssim 45 \text{ km s}^{-1}$ ) single star (see discussion in Murphy & Lawson 2015).

### 2.1 $H\alpha$ emission and accretion

Accretion of gas-rich material from the inner regions of a circumstellar disc onto the star is typically accompanied by enhanced Balmer and other line emission (e.g. Muzerolle, Hartmann & Calvet 1998). The  $H\alpha$  emission observed in WISE J0808–6443 is much larger than typically seen in mid-M field stars and immediately suggests the star is accreting. White & Basri (2003) and Barrado y Navascués & Martín (2003) found that mid-M stars with  $\text{EW}[\text{H}\alpha] < -20 \text{ Å}$  tend to be T-Tauri stars with other corroborating evidence of accretion (strong IR excess, veiling). Similarly, by comparing the *Spitzer* infrared colours of young stars with and without dusty inner discs, Fang et al. (2009) proposed an EW limit of  $-18 \text{ Å}$  for an M5 accretor. Over three nights we measured  $\text{EW}[\text{H}\alpha]$  values in the range  $-125 < \text{EW} < -65 \text{ Å}$ , considerably in excess of these criteria (see Fig. 3).

The width of the  $H\alpha$  line (typically quantified by the velocity full width at 10 per cent of peak flux, or  $v_{10}$ ) is also used to distinguish accretors from stars whose narrower emission is due to chromospheric activity. White & Basri (2003) proposed a limit of  $v_{10} > 270 \text{ km s}^{-1}$  for accretors independent of spectral type, while Jayawardhana, Mohanty & Basri (2003) and Fang et al. (2013) have suggested limits of  $200 \text{ km s}^{-1}$  and  $250 \text{ km s}^{-1}$ , respectively. Fig. 2 shows the  $H\alpha$  line profiles of our four WiFeS spectra. We calculated  $v_{10}$  values by fitting a linear function over  $\pm 500$ – $1000 \text{ km s}^{-1}$  and normalising the spectra, then determining the two velocities at which the flux profile fell to one tenth of its peak value (see Fig. 2). These  $v_{10}$  measurements are given in Table 1 and Fig. 3, and are clearly indicative of accretion.

The variability of the EW and  $v_{10}$  values in Table 1 is commonly seen in other accretors (e.g. Nguyen et al. 2009; Costigan et al. 2012) and probably indicates variability in the accretion rate. Applying the  $v_{10}[\text{H}\alpha]$ – $\dot{M}_{\text{acc}}$  relation of Natta et al. (2004) to our R7000 spectra yields mass accretion rates of  $(1.0$ – $3.3) \times 10^{-10} M_{\odot} \text{ yr}^{-1}$  ( $-10 < \log \dot{M}_{\text{acc}}/M_{\odot} \text{ yr}^{-1} < -9.5$ ), with an uncertainty of 0.4 dex ( $2.5\times$ ). These rates are comparable to those observed in low-mass members of the TW Hydrae associa-

<sup>1</sup> <http://www.diskdetective.org>

**Table 1.** Summary of ANU 2.3-m/WiFeS observations of WISE J080822.18–644357.3.

UT Date	Grating /Dichroic	Spectral Type	RV (km s <sup>-1</sup> )	EW[Li I] (mÅ)	EW[H $\alpha$ ] ( $\pm 5$ Å)	$v_{10}$ [H $\alpha$ ] ( $\pm 10$ km s <sup>-1</sup> )	EW[He I $\lambda$ 5876] (Å)	EW[He I $\lambda$ 6678] (Å)
2017 Jan 7	R7000/RT480	M4 (veiled?) <sup>a</sup>	25.7 $\pm$ 1.9 <sup>d</sup>	300 $\pm$ 50	-110	352	-7.5	-2.7
2017 Jan 9	R7000/RT480	M4.5 <sup>a</sup>	22.3 $\pm$ 1.6 <sup>d</sup>	400 $\pm$ 30	-125	332	-5.3	-1.8
2017 Feb 6	R7000/RT480	M4.5 <sup>a</sup>	22.5 $\pm$ 0.5 <sup>d</sup>	390 $\pm$ 30	-65	298	-6.4	-1.5
2017 Feb 6	R3000/RT560	M5 <sup>b</sup> , M4.8 $\pm$ 0.2 <sup>c</sup>	...	...	-75	419	-7.5	-3.3

<sup>a</sup> Based on comparison to SDSS M dwarf templates over 5300–7000 Å.

<sup>b</sup> Based on comparison to SDSS M dwarf templates over 5500–9200 Å.

<sup>c</sup> Average of R1, R2, R3, TiO8465, c81 and VO2 molecular indices, as calibrated by [Riddick, Roche & Lucas \(2007\)](#).

<sup>d</sup> Mean and standard deviation of velocities calculated from 14 (January) and 4 (February) M-type standards.

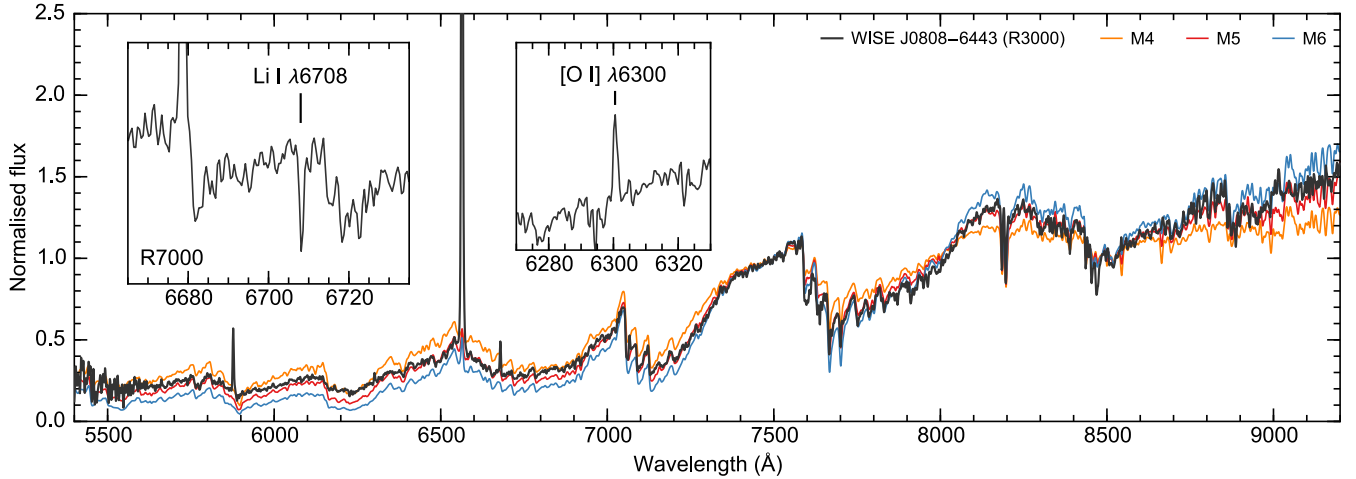


**Figure 1.** Telluric-corrected WiFeS/R3000 spectrum of WISE J0808–6443 compared to the SDSS average M dwarf templates of [Bochanski et al. \(2007\)](#). Both the WiFeS and SDSS spectra were smoothed and normalised at 7500 Å prior to plotting. Strong H $\alpha$ , He I  $\lambda$ 5876 and  $\lambda$ 6678 emission is apparent, as well as prominent Na I absorption at 8200 Å. On this scale the H $\alpha$  line continues to a peak flux of 4.85 (see also Fig. 2). The insets show the region around the Li I  $\lambda$ 6708 youth indicator and [O I]  $\lambda$ 6300 emission in the higher-resolution 2017 February 6 R7000 spectrum. Note also the strong He I  $\lambda$ 6678 emission.

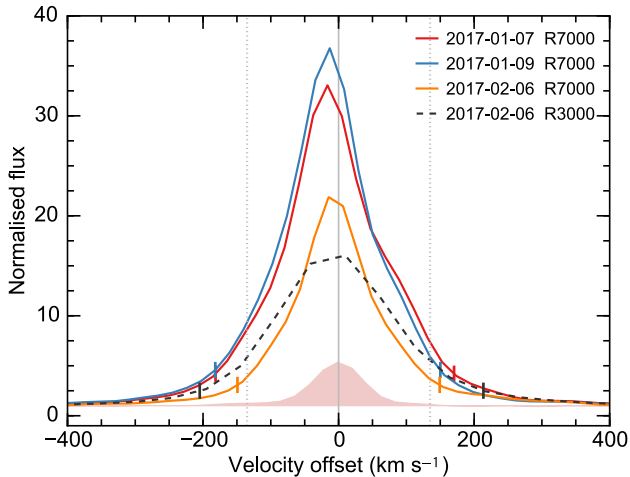


**Figure 2.** WiFeS H $\alpha$  velocity profiles of WISE J0808–6443. All spectra have been shifted to the heliocentric rest frame. Vertical markers show the velocities at which the flux is 10 per cent of the peak value. The two dotted lines are the (symmetric)  $v_{10} = 270$  km s<sup>-1</sup> accretion criterion of [White & Basri \(2003\)](#). For comparison, the shaded region shows the H $\alpha$  profile of the new M5 TW Hydrae association member and non-accretor TWA 36 (EW = -9.5 Å,  $v_{10} = 169$  km s<sup>-1</sup>; [Murphy, Lawson & Bento 2015](#)).

tion,  $\eta$  Cha cluster and Scorpius-Centaurus OB association ([Muzerolle et al. 2000](#); [Lawson, Lyo & Muzerolle 2004](#); [Murphy, Lawson & Bento 2015](#)) and are 1–2 orders of magnitude below those typi-

cally inferred in young star-forming regions such as Taurus and  $\rho$  Ophiuchus (e.g. [Calvet, Hartmann & Strom 2000](#)). We note that the [Natta et al. \(2004\)](#) relation was determined from a sample of few Myr-old stars and is not strictly applicable to older pre-MS stars, whose radii will be smaller and surface gravities higher. For example, assuming a constant accretion luminosity  $L_{\text{acc}}$ , the radius and hence mass accretion rate  $\dot{M}_{\text{acc}} \propto L_{\text{acc}} R_{\star} / GM_{\star}$  onto a  $0.1 M_{\odot}$  star is  $\sim 4\times$  (0.6 dex) smaller at an age of 40 Myr compared to 2 Myr ([Feiden 2016](#)). The accretion rates derived above do not include any corrections for age.

## 2.2 Lithium depletion and low-gravity features

Because lithium is easily destroyed in stellar interiors, with some caveats the presence of Li I  $\lambda$ 6708 absorption in a star is a sign of youth. As young stars contract toward the main-sequence, their core temperatures rise until at  $\sim 3 \times 10^6$  K lithium burns. These temperatures can be reached in either fully-convective mid- to late-M dwarfs or at the base of the convective zone in late-K or early-M dwarfs. Between these luminosities, rapid depletion ensues and the Li I  $\lambda$ 6708 feature is no longer visible. This mass-dependent behaviour leads to the depletion patterns seen in Fig. 4, where we plot the EW[Li] of WISE J0808–6443 compared to young moving group members from the literature. Based on the moderate amount of depletion observed in the star, we can immediately infer that it is older than the  $\sim 10$  Myr TW Hydrae association (TWA), whose mid-M members are essentially undepleted.

The Carina association is believed to be part of a larger com-

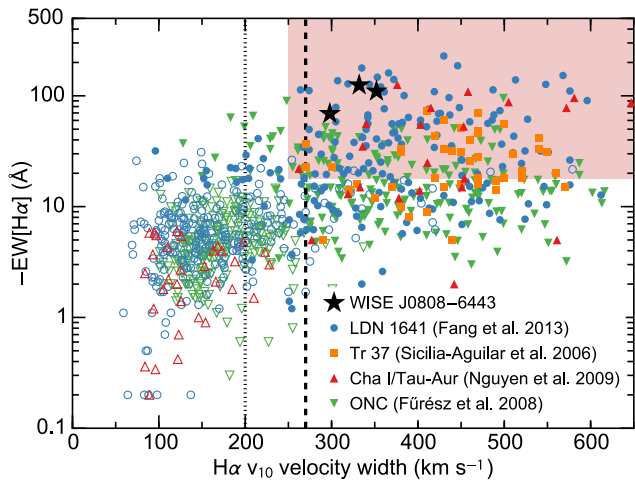


**Figure 3.** EW[H $\alpha$ ] and  $v_{10}$ [H $\alpha$ ] measurements for WISE J0808–6443 compared to members of young clusters and star-forming regions; LDN 1641 (Fang et al. 2013), Trumpler 37 (Sicilia-Aguilar et al. 2006), Cha I and Taurus-Auriga (Nguyen et al. 2009) and the Orion Nebula Cluster (Fűrész et al. 2008). Filled points are accretors with confirmed inner discs from *Spitzer*, open points are non-accretors. The dotted and dashed lines mark the  $v_{10}$  accretion criteria proposed by Jayawardhana et al. (2003) and White & Basri (2003), respectively, while the shaded region shows the criteria for an M5 accretor proposed by Fang et al. (2009, 2013).

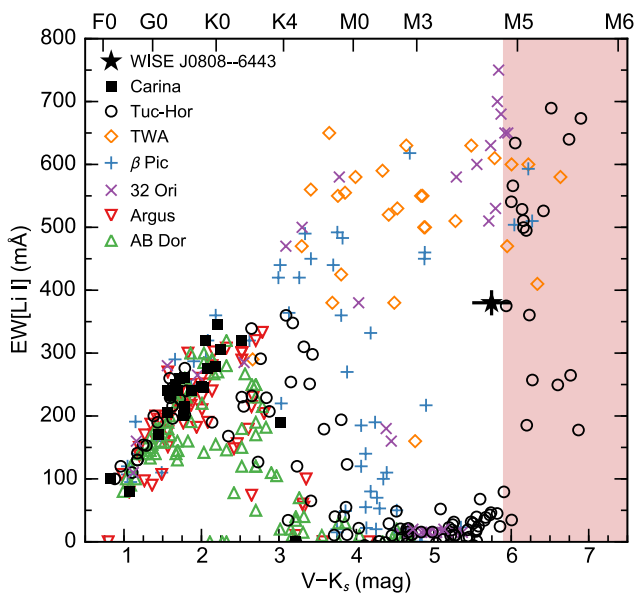


**Figure 4.** EW[Li I] of WISE J0808–6443 compared to other young moving group members, compiled from the studies of da Silva et al. (2009), Schneider et al. (2012), Kraus et al. (2014), Malo et al. (2014b), Binks & Jeffries (2016) and Bell et al. (2017). For WISE J0808–6443 we assume an uncertainty of 0.2 mag on its faint SPM4 V-band magnitude. The shaded region denotes the Li-rich side of the Tuc-Hor lithium depletion boundary.

plex (the so-called Great Austral Young Association or GAYA; Torres et al. 2001, 2008) comprising itself and the Columba and Tucana-Horologium associations. Although spatially and kinematically distinct, Bell, Mamajek & Naylor (2015) found that all three associations are co-eval, with ages of  $\sim 45$  Myr. Unlike Carina, which is a particularly sparse association of a few dozen high-probability members (see Section 3.1), Tuc-Hor contains hundreds of stars (Kraus et al. 2014). This census provides a well-sampled depletion pattern for stars at age  $\sim 45$  Myr and we may use this to assess whether the Li depletion of WISE J0808–6443 is consistent with such an age. From Fig. 4 it is clear that WISE J0808–6443 oc-

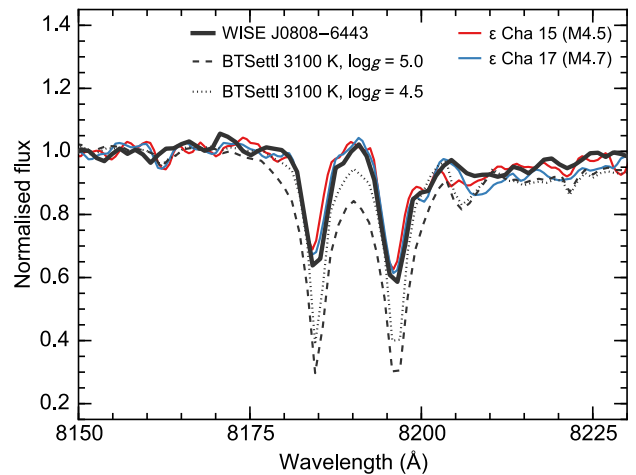


**Figure 5.** WiFeS/R3000 spectrum around the 8200 Å Na I doublet. The strength of Na I absorption is similar to members of the young  $\epsilon$  Cha association (Murphy et al. 2013). Also plotted are two 3100 K BT-Settl-CIFIST model atmospheres (Baraffe et al. 2015), smoothed to  $R \approx 3000$  and placed on the same wavelength scale as WISE J0808–6443. The absorption in WISE J0808–6443 is much weaker than the  $\log g = 5.0$  model, particularly in the broad line wings, but similar to the  $\log g = 4.5$  spectrum.

cupies a region between the Li-poor early M-type Tuc-Hor members and the Li-rich mid to late M-type members. This sharp discontinuity (see the shaded region of Fig. 4) defines the lithium depletion boundary (LDB) of the association and its luminosity provides a precise, almost model-independent age of  $40 \pm 3$  Myr (Kraus et al. 2014). The position of WISE J0808–6443 in Fig. 4 is entirely consistent with the expected LDB position for a co-eval population of nominal age 40–45 Myr. A strong upper age limit is provided by the 80–90 Myr LDB age of the  $\alpha$  Persei cluster, whose LDB occurs at a spectral type of M6–6.5 (Stauffer et al. 1999; Barrado y Navascués, Stauffer & Jayawardhana 2004).

As the radius of a star decreases during its pre-MS evolution, surface gravity-sensitive absorption features, such as those of the alkali metals or metal hydrides, can be used as indicators of a star’s youth. At mid-M spectral types, one of the best gravity-sensitive features is the Na I doublet at  $\lambda 8183/8195$  (Schlieder et al. 2012). While the Na I line strength can not provide a precise estimate of age, it has been widely used to distinguish young cluster members from giants and Gyr-old field stars (e.g. Slesnick, Carpenter & Hillenbrand 2006). We plot in Fig. 5 the region around the Na I doublet for WISE J0808–6443 and two members of the 3–5 Myr-old  $\epsilon$  Cha association of similar spectral type, observed with the same instrument settings (Murphy et al. 2013). The strength of the absorption in WISE J0808–6443 (EW[Na I]  $\approx 4$  Å) is very similar to the two young stars, and is much weaker than a dwarf model atmosphere of similar temperature. This shows that WISE J0808–6443 has a weaker surface gravity and hence younger age than a field M dwarf.

In light of its strong H $\alpha$  emission, lithium absorption and low gravity, we spectroscopically classify WISE J0808–6443 as an accreting, Classical T-Tauri Star (CTTS).

### 3 PROPER MOTION AND KINEMATICS

Silverberg et al. (2016) assigned WISE J0808–6443 as a candidate member of the Carina association based entirely on its position and SPM4 proper motion, considering no other astrometric catalogues. The SPM4 proper motion has large uncertainties ( $\sim 7$  mas yr $^{-1}$ ) and so a critical examination of other proper motion measurements and an independent estimate is warranted. Table 2 lists the published proper motions for WISE J0808–6443 and our

**Table 2.** Estimated proper motions for WISE J080822.18–644357.3.

Reference	$\mu_{\alpha} \cos \delta$ (mas yr <sup>-1</sup> )	$\mu_{\delta}$ (mas yr <sup>-1</sup> )
SuperCOSMOS (Hambly et al. 2001)	$-6.8 \pm 4.8$	$18.5 \pm 4.9$
USNO-B1.0 (Monet et al. 2003)	$0 \pm 0$	$0 \pm 0$
PPMXL (Röser et al. 2010)	$-11.2 \pm 8.5$	$17.8 \pm 8.5$
SPM4 <sup>a</sup> (Girard et al. 2011)	$-9.9 \pm 7.1$	$36.7 \pm 7.1$
AllWISE (Cutri et al. 2014)	$53 \pm 27$	$-14 \pm 27$
HSOY (Altmann et al. 2017)	$-14.0 \pm 3.1$	$27.9 \pm 3.1$
This work <sup>b</sup>	$-12.5 \pm 1.9$	$29.4 \pm 2.2$
This work (adopted) <sup>c</sup>	$-12.5 \pm 2.1$	$29.4 \pm 2.5$

<sup>a</sup> Value adopted by Silverberg et al. (2016).

<sup>b</sup> Based on a simple least-squares fit.

<sup>c</sup> Calculated as in <sup>b</sup>, but multiplies the uncertainty by a ratio taking into account the  $\chi^2$  of the fit.

new measurement (see below). Notably, the star does not appear in any UCAC catalogue (including UCAC5). It is apparent that the proper motion of WISE J0808–6443 is not well constrained, with large differences between catalogues (e.g.  $\Delta\mu_{\delta} \approx 19$  mas yr<sup>-1</sup> between SPM4 and PPMXL; Röser, Demleitner & Schilbach 2010). Furthermore, the USNO B1.0 catalogue (Monet et al. 2003) lists a proper motion of zero for this star, which signifies it was unable to detect a statistically significant proper motion. Given the ambiguity with regards to its proper motion, to assign membership of WISE J0808–6443 – and by extension an age – on the basis of a single poorly-constrained observable is clearly insufficient.

We calculated a new proper motion for WISE J0808–6443 using the published positions compiled in Table 3 and the least-squares formulae of Teixeira et al. (2000). Given the heterogeneity of the source catalogues and heteroskedasticity of their uncertainties, we assessed the proper motion uncertainties by multiplying the least-squares estimates by their Birge ratios (Mohr & Taylor 2005), in effect forcing the reduced  $\chi^2$  of the linear astrometric fits to be  $\sim 1$ . As seen in Table 2, the differences in proper motion uncertainties between the simple least squares estimates and the Birge ratio-adjusted estimates are negligible. We adopt the latter for the kinematic calculations described below. Our new proper motion agrees with SPM4 to within the latter’s larger uncertainties and is similar to values recently published in the HSOY catalogue (Altmann et al. 2017, see Table 2), which was formed by combining *Gaia* DR1 astrometry (Gaia Collaboration et al. 2016) with PPMXL.

### 3.1 Young moving group membership

With our revised proper motion and radial velocity measurement we can better test the membership of WISE J0808–6443 in Carina or another of the young moving groups which populate the Solar neighbourhood. The BANYAN II Bayesian membership tool (v1.4) now returns a membership probability for Carina of 91.7 per cent (assuming  $< 1$  Gyr age priors) at an inferred distance of  $83 \pm 7$  pc. This is comparable to the 93.9 per cent probability reported by Silverberg et al. at  $65^{+9}_{-8}$  pc using just the SPM4 proper motion. No other young group tested by BANYAN (TW Hya,  $\beta$  Pic, Columba, Tuc-Hor, Argus, AB Dor) returned a non-zero membership probability, with the balance of probabilities going to the young field hypothesis. To investigate the robustness of the BANYAN results, we also tested the literature proper motions from Table 2. All returned most-likely memberships in either Carina (SPM4: 98 per cent, HSOY: 93 per cent) or the young field population (SuperCOSMOS, AllWISE, PPMXL). In the latter case, the balance of membership probabilities always went to Carina ( $P_{\text{Car}} = 1.5, 3.8$  and  $32.5$  per cent, respectively). No other group returned a non-zero probability.

Several nearby, young moving groups are not included in BANYAN – we additionally tested membership of WISE J0808–6443 in  $\eta$  and  $\epsilon$  Cha (including ejection from  $\eta$  Cha; Murphy, Lawson & Bessell 2010), Octans and the Lower Cen-Cru subgroup of the Sco-Cen OB association, and could not find a satisfactory kinematic or spatial match (e.g. low membership probabilities, high peculiar motions, predicted radial velocities which disagree with measured value). WISE J0808–6443 is also in the vicinity of the IC 2602 and IC 2391 open clusters, but neither provide a plausible kinematic fit. Carina appears to be the only known group to which WISE J0808–6443 could plausibly belong<sup>2</sup>.

Adopting the Malo et al. (2014a) mean space motion for Carina and our new proper motion for WISE J0808–6443, we use the convergent point method (e.g. Mamajek 2005) to calculate a kinematic parallax ( $\varpi_{\text{kin}} = 11.16 \pm 1.13$  mas;  $d = 90 \pm 9$  pc) and predicted radial velocity ( $21.5 \pm 1.2$  km s<sup>-1</sup>). The larger distance stems from the revised proper motion having a smaller magnitude ( $32$  mas yr<sup>-1</sup>) than the SPM4 value ( $38$  mas yr<sup>-1</sup>). The star’s proper motion is pointing towards Carina’s convergent point, with only  $2.4 \pm 2.2$  mas yr<sup>-1</sup> of peculiar motion. We calculate a heliocentric position of  $(X, Y, Z) = (12.1, -85.4, -25.8) \pm (4.9, 6.3, 4.2)$  pc and a space motion of  $(U, V, W) = (-10.3, -23.8, -5.2) \pm (1.4, 1.1, 1.0)$  km s<sup>-1</sup>, which agrees with the Malo et al. (2014a) mean group velocity at better than  $2$  km s<sup>-1</sup>.

### 3.2 Carina members in the literature

In the top row of Fig. 6 we plot the position and velocity of WISE J0808–6443 against the mean values for young moving groups and associations within 100 pc from Malo et al. (2014a). While there is excellent spatial and kinematic agreement between WISE J0808–6443 and Carina in this diagram, it is important to note that their Carina model is based on only five stars; AB Pic, HD 49855, HD 55279, V479 Car, and HD 83096AB, these being the only stars in the original membership list of Torres et al. (2008) with *Hipparcos* parallaxes. The updated models of Gagné et al. (2014) used by BANYAN II excluded V479 Car and added the nearby M dwarfs GJ 2079 and GJ 1167 (Shkolnik et al. 2012), but with only six systems the mean properties of Carina are poorly defined. We have gathered proposed Carina members from the literature with radial velocities and parallaxes (predominantly new measurements from *Gaia* DR1; Gaia Collaboration et al. 2016) and computed their space motions and positions which are plotted in the bottom row of Fig. 6. These candidates came mainly from the memberships of Torres et al. (2008), Moór et al. (2013) and Elliott et al. (2014, 2016), with additional stars from Viana Almeida et al. (2009), Shkolnik et al. (2012), Riedel et al. (2014) and Bowler et al. (2015). Many of these stars have also been proposed by various authors as members of other young moving groups, especially Columba, with which Carina shares a similar position and velocity (see Fig. 6). For example, Elliott et al. (2014) reclassify seven Torres et al. (2008) members (including all five of the *Hipparcos* stars above) as either Columba members or Carina non-members, although their methodology or rationale is not given.

<sup>2</sup> Since this work was accepted for publication, BANYAN II has been replaced by BANYAN  $\Sigma$  (Gagné et al. 2018), which provides several improvements including spatio-kinematic models for 21 additional young groups aged 1–800 Myr. WISE J0808–6443 now returns a Carina membership probability of 89 per cent at an inferred distance of  $88 \pm 6$  pc, in good agreement with our results above. No other young group returned a non-zero membership probability, with the balance of probabilities going to the field model. The BANYAN  $\Sigma$  kinematic model for Carina contains seven stars – the original membership list of Malo et al. (2014a) in addition to the new K3 member HD 298936 (TWA 21; see Gagné et al. 2017).

**Table 3.** Astrometry used to calculate the proper motion of WISE J080822.18–644357.3.

$\alpha$ (deg.)	$\delta$ (deg.)	$\sigma_\alpha$ (mas)	$\sigma_\delta$ (mas)	Epoch (yr or JD)	Reference
122.0924291146	-64.7325757593	0.407	0.687	2015.0	<i>Gaia</i> DR1 (Gaia Collaboration et al. 2016)
122.0924381	-64.7326092	34	35.8	2010.5589	AllWISE (Cutri et al. 2014)
122.092536	-64.732738	400	400	2450916.764023	DENIS DR3 (Epchtein et al. 1999)
122.092519	-64.732778	400	400	2451237.607512	DENIS DR3 (Epchtein et al. 1999)
122.0925957	-64.7327013	69.5	69.5	2000.0	SPM4 (Girard et al. 2011)
122.092535	-64.732719	330	340	1991.131	GSC2.3.2 (Lasker et al. 2008)
122.092670	-64.732823	66	83	1985.1	USNO-B1.0 (Monet et al. 2003)

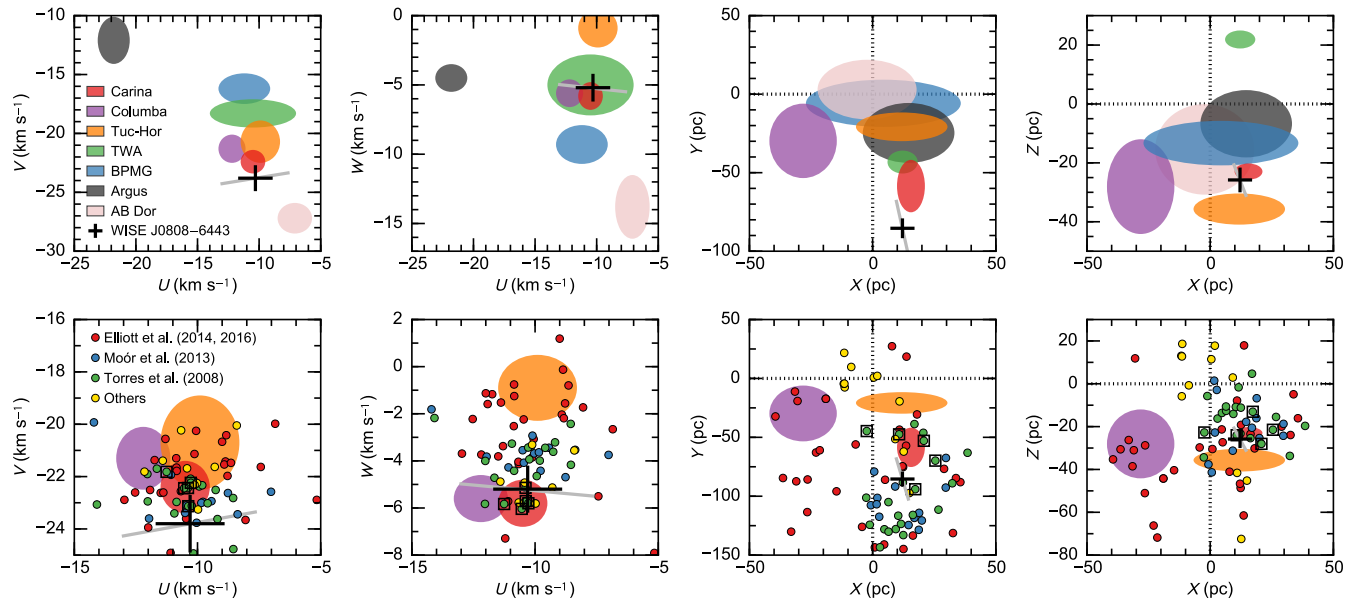


**Figure 6.** *Top row:* Three-dimensional Galactic velocity and position of WISE J0808–6443 relative to several nearby, young moving groups from Malo et al. (2014a). Uncertainties for WISE J0808–6443 were calculated from uncertainties on the proper motion, radial velocity and distance. The grey line shows the change in velocity and position as the  $90 \pm 9$  pc assumed distance changes by  $\pm 2\sigma$ . Based on this comparison, WISE J0808–6443 is a likely Carina member. *Bottom row:* As above, but only showing the Carina, Columba and Tuc-Hor associations. Points are proposed Carina members from the literature with trigonometric parallaxes, predominantly from *Gaia* DR1. The five square markers are the ‘bona fide’ members of Malo et al. (2013, 2014a). These stars were the only Torres et al. (2008) members with *Hipparcos* parallaxes.

The general distribution of Carina candidates in Fig. 6 is spatially and kinematically distinct from both Columba and Tuc-Hor (whose mean phase space positions are much better defined from several tens of members with parallaxes). Carina is clearly much larger than defined by the five *Hipparcos* stars (which do not appear to be Columba members, c.f. Elliott et al. 2014), especially in the negative  $Y$  direction. This is similar to the solution proposed by Torres et al. (2008) with kinematic distances and is understandable as the limited depth of *Hipparcos* would favour nearby stars. Assuming they are all bona fide Carina members, from the 74 stars with parallaxes and radial velocities we calculate a mean space motion of  $(-10.4, -22.2, -3.5) \pm (1.8, 1.4, 1.9) \text{ km s}^{-1}$  ( $1\sigma$  variation), which is  $2.3 \text{ km s}^{-1}$  larger in  $W$  than the Malo et al. (2014a) velocity. If true, the revised space motion does not change our derived 90 pc kinematic distance by more than a parsec.

There are several proposed Carina members in the immediate vicinity of WISE J0808–6443. The Moór et al. (2013) star TYC 8933-1204-1 is only  $1.40^\circ$  away and, while it does not possess a *Gaia* DR1 parallax, its UCAC5 proper motion is only  $5 \text{ mas yr}^{-1}$  from that of WISE J0808–6443 and the stars’ radial velocities agree to  $1 \text{ km s}^{-1}$ . Of the proposed members with parallaxes, the G5 star TYC 8929-927-1 (Torres et al. 2008) is only  $2.07^\circ$  away, with radial velocity  $23.4 \pm 0.5 \text{ km s}^{-1}$  (Torres et al. 2006) and  $\varpi = 10.85 \pm 0.31 \text{ mas}$  ( $d = 92.2 \pm 2.6 \text{ pc}$ ). The star’s *Gaia* proper motion matches that of WISE J0808–6443 to within  $\sim 1 \text{ mas yr}^{-1}$ .

With a projected separation of  $\sim 3.3 \text{ pc}$ , it is unlikely that they are bound, but more likely unbound members of the same young moving group. Given their congruent proper motions, the *Gaia* parallax distance for TYC 8929-927-1 corroborates our kinematic distance of  $90 \pm 9 \text{ pc}$  for WISE J0808–6443. Finally, we note that the Gagné et al. (2015) Carina candidate 2MASS J08045433–6346180 ( $<M2$ ; 99 per cent BANYAN membership probability) is only  $1.03^\circ$  from WISE J0808–6443. Aside from being X-ray bright (1RXS J080455.0–634621), little is known about this star, though given its much larger UCAC5 proper motion it cannot be co-distant with WISE J0808–6443.

While a critical re-evaluation of all proposed Carina members in light of new *Gaia* parallaxes is beyond the scope of this work, given the close spatial and kinematic agreement between WISE J0808–6443 and the stars in Fig. 6, as well as the presence of other proposed Carina members in its vicinity, we see no reason not to assign membership to the association. Unambiguous confirmation, however, will require a refined Carina membership and a trigonometric parallax. *Gaia* should provide a parallax for a  $G = 16$  mag M5 star with an estimated end-of-mission uncertainty of approximately  $45 \mu\text{as}^3$ .

<sup>3</sup> <http://www.cosmos.esa.int/web/gaia/science-performance>

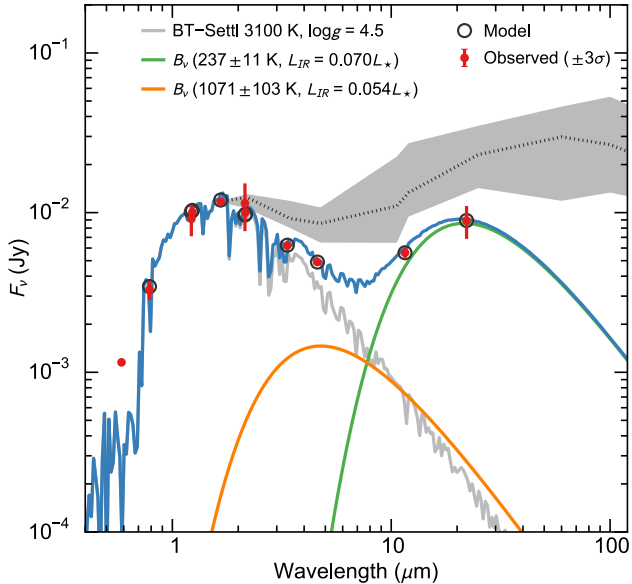


**Figure 7.** Spectral energy distribution of WISE J0808–6443, with photometry from *Gaia*, DENIS, 2MASS and *WISE* plotted in red with their  $3\sigma$  uncertainties. The observed SED (blue line) is approximated by the sum of a 3100 K BT-Settl model and blackbodies of 237 K ( $0.070 L_{\star}$ ) and 1071 K ( $0.054 L_{\star}$ ), fit to the DENIS, 2MASS and *WISE* data. For comparison, the interquartile range of K5–M2 Class I/II Taurus sources from D’Alessio et al. (1999) is given by the shaded region, normalised at  $1.6 \mu\text{m}$ .

#### 4 CIRCUMSTELLAR DISC EMISSION

Silverberg et al. (2016) noted that WISE J0808–6443 has a strong infrared excess in the *WISE* W3 ( $12 \mu\text{m}$ ) and W4 ( $22 \mu\text{m}$ ) bands and fitted the star’s spectral energy distribution (SED) with a 2900 K stellar atmosphere and  $\sim 260$  K blackbody of luminosity  $L_{\text{IR}}/L_{\star} = 0.081$ . In this section we re-examine the infrared excess using models and photometry provided by the Virtual Observatory SED Analyzer (VOSA v5.1; Bayo et al. 2008).

Within VOSA we first gathered all available photometry for WISE J0808–6443 from photometric catalogues. The resulting SED contained fluxes from *Gaia* DR1 (*G*), DENIS (*iJK*; Epchtein et al. 1999), 2MASS (*JHK<sub>s</sub>*; Cutri et al. 2003) and All*WISE* (*W1–W4*; Cutri et al. 2014). Following Silverberg et al. we fit synthetic photometry derived from solar-metallicity BT-Settl-CIFIST models ( $\Delta T_{\text{eff}} = 100$  K; Baraffe et al. 2015; Allard, Homeier & Freytag 2012), restricting the surface gravity to  $\log g = 4.5$ . The excess finding routine in VOSA identified a possible excess redward of *W1* so in fitting the models we did not include the four *WISE* bands or the broad *Gaia* *G*-band, which may be contaminated by the accretion-driven strong *H $\alpha$*  line or any blue continuum excess<sup>4</sup>. For this reason we also excluded the SPM4 *B*- (photographic) and *V*-band photometry. Furthermore, we do not consider the effects of reddening in this analysis – at a kinematic distance of 80–90 pc, WISE J0808–6443 is expected to lie within the Local Bubble and reddening maps predict its reddening and extinction should be negligible ( $E(b-y) < 0.01$ ,  $A_V < 0.04$  mag; Reis et al. 2011), although we cannot exclude the possibility of residual reddening along the line of sight.

The resulting SED and best-fit photosphere model of  $T_{\text{eff}} = 3100$  K is shown in Fig. 7. This temperature is consistent with the WiFeS M5 spectral type and the corresponding dwarf temperature

<sup>4</sup> By including the *W1* magnitude in the VOSA BT-Settl model fit we were able to replicate the Silverberg et al. results and fit a 2900 K model atmosphere to the (*iJK*)<sub>DENIS</sub>*JHK<sub>s</sub>* *W1* photometry. However, the  $\chi^2$  of this fit was much larger than the 3100 K fit obtained in this study.

**Table 4.** Infrared excesses for WISE J080822.18–644357.3, assuming the intrinsic colours of a pre-MS M5 star from Pecaut & Mamajek (2013). Almost identical excesses are obtained using the main-sequence colours.

$E(K_s - W1)$ (mag)	$E(K_s - W2)$ (mag)	$E(K_s - W3)$ (mag)	$E(K_s - W4)$ (mag)
$0.102 \pm 0.034$	$0.267 \pm 0.033$	$2.252 \pm 0.039$	$4.017 \pm 0.088$

(3050 K) from Pecaut & Mamajek (2013). The SED  $T_{\text{eff}}$  is  $\sim 200$  K hotter than the corresponding pre-MS temperature (2880 K) from the scale of Pecaut & Mamajek (2013), however their pre-MS sample of mid-M stars was dominated by younger, lower surface gravity stars from the  $\sim 10$ –25 Myr-old  $\eta$  Cha, TW Hya, and  $\beta$  Pic groups. Combining these temperature estimates, we adopt  $T_{\text{eff}} \approx 3050 \pm 100$  K for WISE J0808–6443.

From the SED fit it is clear that, in addition to the *W3* and *W4* bands, there are smaller excesses in both shorter wavelength *WISE* filters. This is also apparent when comparing the observed  $K_s$ –*WISE* colours to the intrinsic colours of an M5 star from Pecaut & Mamajek (2013, see Table 4). We attempted to fit a single blackbody to the infrared excess ( $\sim 470$  K;  $L_{\text{IR}}/L_{\star} = 0.095$ ), but this gave a poor match to the  $22 \mu\text{m}$  data. Although not necessarily a physical model, a simple double blackbody disc with a ‘warm’  $\sim 240$  K outer component having  $L_{\text{IR,warm}}/L_{\star} = 0.070 \pm 0.015$  and a ‘hot’  $\sim 1100$  K inner component with  $L_{\text{IR,hot}}/L_{\star} = 0.054 \pm 0.018$  provides a good fit to the full gamut of *WISE* photometry (see Fig. 7). Together, the fractional luminosity of these components is  $0.12 L_{\star}$  – approximately 50 per cent brighter than the single temperature model of Silverberg et al. (2016). With only four *WISE* fluxes over 3–22  $\mu\text{m}$  (see discussion in Sec. 4.1 below), we made no attempt to fit more complex disc models (e.g. Robitaille 2017), which suffer from degeneracies due to a large number of free parameters (typically 7–12 for the models above).

Assuming large grains are responsible for the infrared excess, these blackbody temperatures correspond to emission radii of  $\sim 25 \mathcal{R}_{\odot}^{\text{N}}$  ( $0.115$  au) and  $1.2 \mathcal{R}_{\odot}^{\text{N}}$  ( $0.0056$  au), respectively (Backman & Paresce 1993). The hot dust at the latter radius is likely associated with the gas feeding the accretion indicated by the *H $\alpha$*  and He I emission lines at the inner edge of the disc. We note that the temperature of the inner component is comparable to the temperatures where amorphous silicates anneal into crystalline form, before these sublimate at 1300–1400 K (Henning & Meeus 2009). Also, given the star’s size and approximate density ( $\sim 5.6 \text{ g cm}^{-3}$ ), orbiting bodies with densities of  $\sim 1$ – $2 \text{ g cm}^{-3}$  would have Roche limits of  $1.0$ – $1.3 \mathcal{R}_{\odot}^{\text{N}}$ , indicating that the dust could be produced by disrupted planetesimals on trajectories taking them too close to the star. The cooler dust belt seems analogous to the ‘warm dust temperature’ debris discs with characteristic temperatures of  $\sim 190$  K commonly seen among stars ranging from B- through K-type, and likely represents populations of small dust grains sublimating ice from icy planetesimals (Morales et al. 2011, 2016).

#### 4.1 Evolutionary status of the disc

A number of classification schemes have been proposed for the evolutionary stages of circumstellar discs. We adopt the nomenclature of Espaillat et al. (2012), which has also been used by Luhman & Mamajek (2012) and Esplin, Luhman & Mamajek (2014) in their studies of Upper Scorpius and Taurus, respectively. In this scheme *full discs* are optically thick at near- and mid-infrared wavelengths and have not been significantly cleared of primordial dust and gas;

<sup>5</sup>  $\mathcal{R}_{\odot}^{\text{N}} = 695,700 \text{ km}$  = nominal solar radius following IAU 2015 Resolution B3 (Mamajek et al. 2015a).

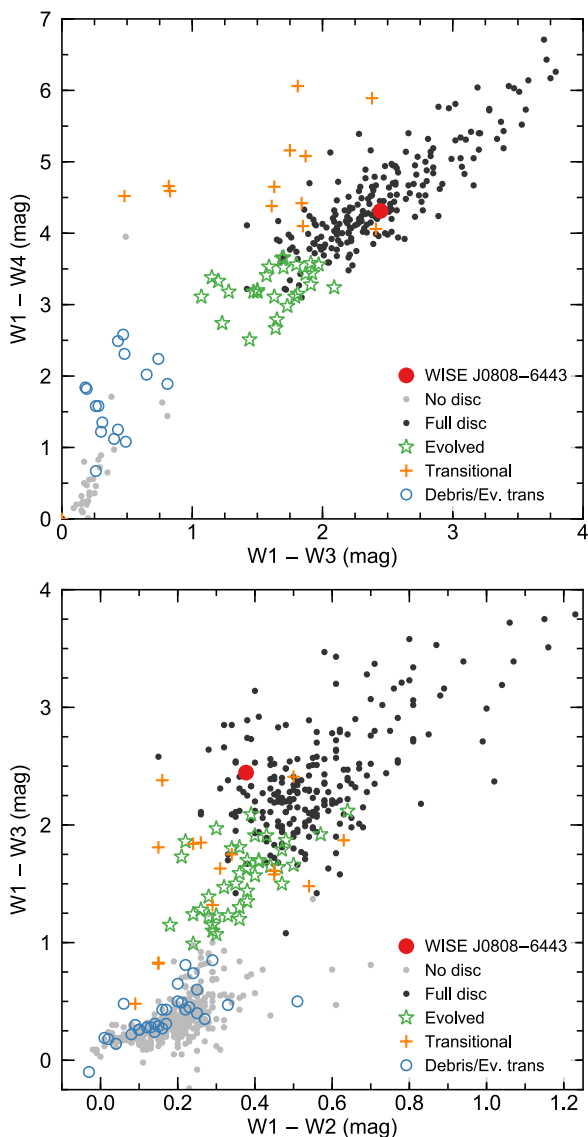


**Figure 8.** AllWISE colour-colour diagrams comparing WISE J0808–6443 to M dwarf (predominantly M4–M6) members of the Taurus and Upper Sco star-forming regions from the studies of [Esplin et al. \(2014\)](#) and [Luhman & Mamajek \(2012\)](#), respectively. The evolutionary state of each disc is given by the symbol shape in the legend.

*pre-transitional* ([Espaillat et al. 2007](#)) and *transitional discs* have large inner gaps or holes, respectively; *evolved discs* (sometimes called anemic or homologously-depleted discs) are becoming optically thin but do not possess large holes or gaps, while *evolved transitional discs* are optically thin and have large holes. All of the above classifications can be considered *primordial discs*, whereas *debris discs* are composed of second-generation dust generated by collisions of planetesimals after the primordial disc has dissipated.

These classes are mapped to AllWISE colours in Figure 8, where we show the classifications of Upper Scorpius and Taurus M dwarfs from [Luhman & Mamajek \(2012\)](#) and [Esplin et al. \(2014\)](#). Moving from red to blue there is a clear evolutionary sequence from full to evolved to debris discs. However, it is important to note that both studies used *Spitzer*/IRAC 8  $\mu\text{m}$  photometry in addition to *WISE* to separate transitional from full discs, which remain somewhat degenerate in Figure 8. From its location in this diagram one could classify WISE J0808–6443 as hosting a full disc without significant clearing of its primordial material and a continuous distribution of dust emitting from the sublimation temperature outwards. However, the SED of the star ap-

pears somewhat evolved compared to the median of Class I/II (full disc) sources in Taurus reported by [D’Alessio et al. \(1999\)](#), (dotted line in Fig. 7) and is well-fit by a double blackbody model with a hot inner disc and cooler outer disc. In the absence of flux measurements between *W2* (4.6  $\mu\text{m}$ ) and *W3* (12  $\mu\text{m}$ ), we cannot definitively distinguish between a full/continuous disc or a (pre-)transitional disc with optically thick inner and outer components separated by an optically thin gap. Irrespective of the final classification, the AllWISE colours, large fractional luminosity and the detection of ongoing accretion indicate a primordial circumstellar disc and rule out WISE J0808–6443 hosting a debris disc, as proposed by [Silverberg et al. \(2016\)](#).

## 4.2 Mid-infrared variability

Both the *W1* and *W2* photometry is listed in AllWISE as exhibiting strong variability (flag `var` = 9900)<sup>6</sup>. This is illustrated in Fig. 9 where we plot  $\sim 300$  individual epoch magnitudes for both the AllWISE and reactivated NEOWISE ([Mainzer et al. 2014](#)) missions. The variation in *W1* and *W2* is extremely well-correlated (Pearson  $r \approx 0.9$ ) and much larger than both the typical uncertainties on a single measurement and the mean AllWISE photometry used in the SED fit. We could find no obvious periodicity in the time series, although the *WISE* sampling (few day observing blocks every six months) are not conducive to this. The smaller ( $N \approx 40$ ) sample of *W3* and *W4* data show no obvious variability or correlation. Similar variability has been observed with *Spitzer* in younger disc-bearing stars (e.g. NGC 2264; [Cody et al. 2014](#)) and can be attributed to various physical processes depending on the light curve morphology, including variable circumstellar obscuration, accretion instabilities, rotating star spots and structural changes in the disc. In this case the rapid ( $\sim 1$  day), semi-periodic variation suggests it is driven by changes in the stellar flux modulated by rotation (e.g. cool/hot spots, obscuration) reprocessed into the infrared and not intrinsic changes in the disc, which should occur on longer timescales. The light curve can also be approximated as the luminosity of the inner blackbody varying at fixed temperature (see Fig. 9), perhaps reflecting the amount of dust in a clumpy inner disc.

## 5 ISOCHRONAL AGE OF WISE J0808–6443

Integrating the 3100 K BT-Settl model atmosphere to 1000  $\mu\text{m}$  we find  $\log(L/L_{\odot}^N) = -2.15 \pm 0.08$  dex at a distance of  $90 \pm 9$  pc, in agreement with the  $\log(L/L_{\odot}^N) = -2.17 \pm 0.10$  dex obtained using the 2MASS *J*-band magnitude and the relation between  $T_{\text{eff}}$  and the *J*-band bolometric correction given in [Pecaut & Mamajek \(2013\)](#)<sup>7</sup>. The estimated effective temperature ( $3050 \pm 100$  K) and bolometric luminosity of the star are consistent with a stellar radius of  $R_{\star} = 0.30 \pm 0.04 R_{\odot}^N$ . In Fig. 10 we plot Hertzsprung-Russell (H-R) diagrams for WISE J0808–6443 against the evolutionary tracks of solar metallicity stars from [Baraffe et al. \(2015\)](#) (BHAC15), MESA Isochrones and Stellar Tracks (MIST) v1.1 ([Dotter 2016](#); [Choi et al. 2016](#)), the Pisa group ([Tognelli et al. 2011](#), extended

<sup>6</sup> The *W1* and *W2* bands are also flagged as possibly contaminated by diffraction spikes from two bright stars approximately 6 arcmin to the south east and south west (flag `cc_flags` = dd00). Visual inspection of the AllWISE Atlas images shows the photometry is unlikely to be affected.

<sup>7</sup> The recent IAU 2015 Resolution B2 regarding the IAU bolometric magnitude scale ([Mamajek et al. 2015b](#)) suggests an adopted  $M_{\text{bol},\odot}$  of 4.74 mag. This differs from the value adopted by [Pecaut & Mamajek \(2013\)](#) by  $-0.015$  mag. To conform with the new resolution and place the luminosity of WISE J0808–6443 on the 2015 IAU scale, we have modified the *J*-band bolometric correction from [Pecaut & Mamajek](#) accordingly.

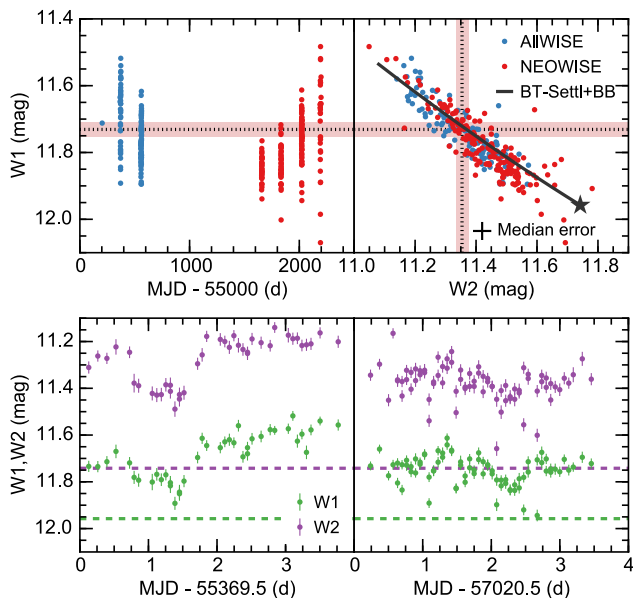


**Figure 9.** *Top left:* W1 individual epoch photometry for WISE J0808–6443 from both the AllWISE and reactivated NEOWISE (Mainzer et al. 2014) missions. *Top right:* Correlation of W1 and W2 magnitudes. The black line shows the expected relation for a 3100 K BT-Settl model combined with a 1071 K blackbody which varies in flux from zero (filled star) to  $0.11 L_{\star}$ . The dotted lines are the mean AllWISE magnitudes used in the SED fit ( $W1 = 11.731 \pm 0.022$  mag,  $W2 = 11.354 \pm 0.020$  mag). *Bottom:* W1 and W2 time series for two four day windows in 2010 and 2014/15. The dashed lines are the photospheric contribution calculated from the BT-Settl model and correspond to the filled star in the upper right plot.

down to  $0.08 M_{\odot}$ ) and the recent magnetic models of Feiden (2016) (also see Malo et al. 2014b). The latter were computed assuming the surface gas pressure is in equilibrium with the magnetic field pressure and adopt an equipartition magnetic field strength equal to the value at 50 Myr (typically a few kG). This is an approximation since the surface gas pressure changes as the object contracts with time, and hence if WISE J0808–6443 is significantly younger than 50 Myr the magnetic field strengths will be overestimated and for older ages slightly underestimated.

The BHAC15, MIST and Pisa models yield ages of 23, 33 and 18 Myr, respectively, all with masses  $\sim 0.1 M_{\odot}$ , while the magnetic models favour an older age ( $\sim 60$  Myr; similar to the assumed 50 Myr equipartition age) and larger mass ( $0.15 M_{\odot}$ ). Bisecting these is the  $45^{+11}_{-7}$  Myr isochronal age of Carina found by Bell et al. (2015) from 12 members and the BHAC15, Pisa, Dartmouth (Dotter et al. 2008) and PARSEC (Bressan et al. 2012) models. Although WISE J0808–6443 is slightly cooler than the least-massive  $0.1 M_{\odot}$  Dartmouth evolutionary track, its  $1\sigma$  error ellipse falls inside the grid and we estimate an age of  $\sim 23$  Myr. Similarly, we find an age of  $\sim 30$  Myr using the older but commonly-cited isochrones of Siess, Dufour & Forestini (2000). The WISE J0808–6443 error ellipse does not overlap the PARSEC v1.1 models at all, while the newest 1.2S version implies a much larger age of 100–200 Myr and mass  $\sim 0.25 M_{\odot}$ . These models were substantially updated for low-mass dwarfs by Chen et al. (2014), who implemented  $T - \tau$  relations from the BT-Settl model atmospheres as surface boundary conditions, calibrated to reproduce the observed mass-radius relation of low-mass dwarfs. Kraus et al. (2015) have suggested that this may be an over-correction in the pre-MS regime, as expected if the recalibration is primarily due to missing opacities which are more important at higher gravities. From the four sets of models in Fig. 10 we calculate a mean isochronal age for WISE J0808–6443 of  $33^{+25}_{-15}$  Myr, in agreement with the isochronal age of Carina. Regardless of the exact age adopted and despite recent revisions to

**Table 5.** Summary of WISE J080822.18–644357.3 parameters.

Parameter	Value	Units
Right Ascension	122.0924291	$^{\circ}$ ( <i>Gaia</i> )
Declination	−64.7325757	$^{\circ}$ ( <i>Gaia</i> )
Spectral type	M5	
$T_{\text{eff}}$	$3050 \pm 100$	K
$\mu_{\alpha} \cos \delta$	$-12.5 \pm 2.1$	$\text{mas yr}^{-1}$
$\mu_{\delta}$	$+29.4 \pm 2.5$	$\text{mas yr}^{-1}$
RV	$22.7 \pm 0.5$	$\text{km s}^{-1}$
Distance	$90 \pm 9$	pc
EW[Li I]	$380 \pm 20$	$\text{m}\text{\AA}$
$\log(L/L_{\odot}^{\text{N}})$	$-2.15 \pm 0.08$	dex
Radius	$0.30 \pm 0.04$	$\mathcal{R}_{\odot}^{\text{N}}$
Mass <sup>a</sup>	$0.16^{+0.03}_{-0.04}$	$M_{\odot}$
Age	$45^{+11}_{-7}$ (Carina)	Myr
	$33^{+25}_{-15}$ (isochronal)	Myr
( <i>U</i> , <i>V</i> , <i>W</i> )	(−10.3, −23.8, −5.2)	$\text{km s}^{-1}$
	$\pm(1.4, 1.1, 1.0)$	
( <i>X</i> , <i>Y</i> , <i>Z</i> )	(12.1, −85.4, −25.8)	pc
	$\pm(4.9, 6.3, 4.2)$	
$T_{\text{disc, hot}}$	$1071 \pm 103$	K
$L_{\text{disc, hot}}$	$0.054 \pm 0.018 [0..0.11]^b$	$L_{\star}$
$T_{\text{disc, warm}}$	$237 \pm 11$	K
$L_{\text{disc, warm}}$	$0.070 \pm 0.015$	$L_{\star}$

<sup>a</sup> Mass inferred from HR diagram position, interpolating from the evolutionary tracks of Feiden (2016).

<sup>b</sup> Approximate range from variability observed in W1 and W2 photometry (see Fig. 9).

young cluster ages (Bell et al. 2013), WISE J0808–6443 appears to be several times older than typically-quoted circumstellar disc and accretion lifetimes (see Introduction).

## 6 CONCLUSIONS

The parameters of WISE J0808–6443 determined in this work are summarised in Table 5. Based on all available spectroscopy, photometry and astrometry, we conclude the star is a  $\sim 45$  Myr-old M5 ( $\sim 0.1 M_{\odot}$ ) member of the Carina association at a distance of  $\sim 90$  pc and is actively accreting from a gas-rich circumstellar disc.

While rare, the discovery of an accreting low-mass star in the GAYA (Carina, Columba, Tuc-Hor) complex is not unprecedented. Reiners (2009) describe a Li-rich M7.5 star with strong, asymmetric H $\alpha$  emission which they attribute to accretion ( $\log \dot{M}_{\text{acc}}/M_{\odot} \approx -10.9$ ). Their tentative membership assignment to the Tuc-Hor association was confirmed by Gagné et al. (2014). Recently, Boucher et al. (2016) reported finding two brown dwarfs in Columba and Tuc-Hor which host circumstellar discs and show signs of accretion (H $\alpha$ , Pa $\beta$  emission, respectively). The  $0.15 L_{\star}$  fractional disc luminosity of their Tuc-Hor member is similar to the value we find for WISE J0808–6443 and is typical of primordial or early pre-transitional discs. The discovery of these older, low-mass accretors in nearby moving groups could be an indication that at least some low-mass stars and brown dwarfs are able to retain their gas reservoirs *much* longer than previously recognised. Alternatively, some transient mechanism, for example the tidal disruption of inner gas-giant planets or the collisional grinding and accreting of icy comets, may be responsible for generating short-lived, gas-rich discs during the later stages of pre-MS evolution. (e.g. Melis et al. 2012)

Finally, the existence of a  $\sim 45$  Myr-old accreting M dwarf expands the parameter space for investigations of planet formation around low-mass stars. Giant planets are observed less frequently in orbit around M dwarfs (Johnson et al. 2010) and this deficiency is often attributed to the inability of core accretion to build up a large

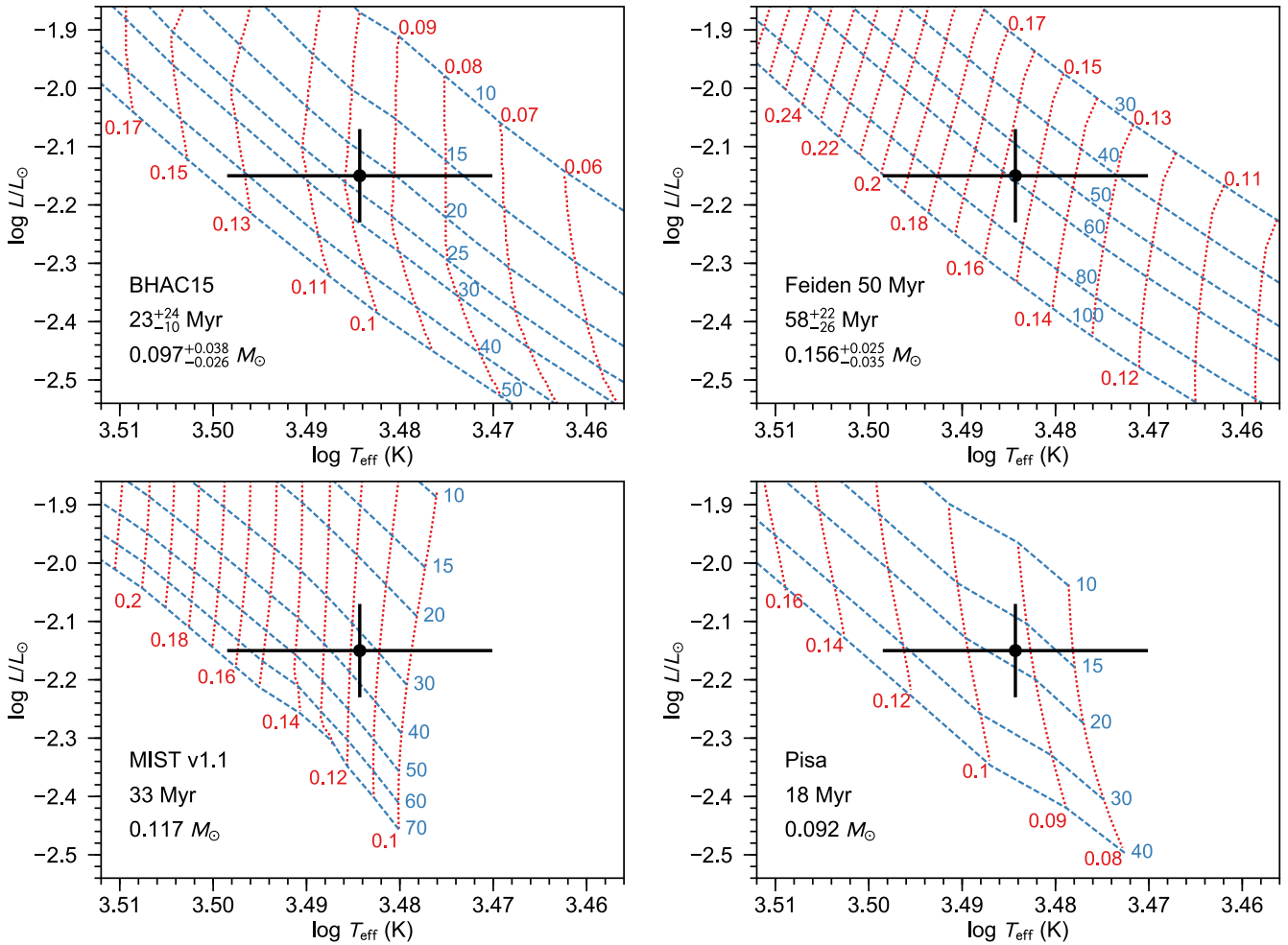


**Figure 10.** H-R diagram position for WISE J0808–6443, with isochrones and evolutionary tracks for solar metallicity pre-MS stars from Baraffe et al. (2015) (top left), 50 Myr magnetic field equipartition models based on Feiden (2016) (top right), MIST v1.1 (bottom left, Dotter 2016; Choi et al. 2016) and the Pisa models of Tognelli et al. (2011) (bottom right). Interpolating at the position of WISE J0808–6443 we estimate ages from these models of  $23^{+24}_{-10}$  Myr,  $58^{+22}_{-26}$  Myr, 33 Myr and 18 Myr, respectively. Uncertainties on the BHAC15 and Feiden age and mass estimates are the 68 per cent confidence intervals and were calculated from a Monte Carlo simulation assuming the quoted uncertainties on  $T_{\text{eff}}$  and  $\log(L/L_{\odot}^{\text{N}})$ .

enough mass within the <10 Myr lifetime of a typical disc (Laughlin, Bodenheimer & Adams 2004). The presence of long-lived gas in the disc could contribute multiple important effects to the star’s growing planetary system, such as (1) prolonged accretion of H and He onto the envelopes of growing proto-planets, (2) prolonged gas-drag which could dampen the eccentricities of growing planetesimals and planets, (3) a prolonged epoch of disc torques which may lead to planet migration, or the formation of planets from matter shepherded by moving secular resonances (e.g. Raymond, Barnes & Mandell 2008; Ogihara & Ida 2009). Finally, the characteristics of the lowest mass pre-MS stars like WISE J0808–6443 and their circumstellar material can also provide important constraints on the conditions that spawn compact systems of small planets in mean-motion resonances orbiting closely around some low-mass stars (e.g. TRAPPIST-1; Gillon et al. 2016).

## ACKNOWLEDGEMENTS

The authors wish to thank Joao Bento (ANU) for the loan of observing time to obtain the R3000 spectrum, Grant Kennedy (Cambridge) for fruitful discussions concerning the circumstellar disc excess, Greg Feiden (North Georgia) for calculating new magnetic evolutionary tracks and the anonymous referee for a prompt and thorough review of the manuscript. SJM acknowledges sup-

port from a University of New South Wales Vice Chancellor’s Fellowship. EEM acknowledges support from the NASA NExSS program. Part of this research was carried out at the Jet Propulsion Laboratory, California Institute of Technology, under a contract with NASA. This publication makes use of VOSA, developed under the Spanish Virtual Observatory project supported from the Spanish MICINN through grant AyA2011-24052. This work has made use of data from the European Space Agency (ESA) mission *Gaia* (<http://www.cosmos.esa.int/gaia>), processed by the *Gaia* Data Processing and Analysis Consortium (DPAC). This publication makes use of data products from the *Wide-field Infrared Survey Explorer*, which is a joint project of the University of California, Los Angeles, and the Jet Propulsion Laboratory/California Institute of Technology, and NEOWISE, which is a project of the Jet Propulsion Laboratory/California Institute of Technology. WISE and NEOWISE are funded by NASA.

## REFERENCES

- Allard F., Homeier D., Freytag B., 2012, *Philosophical Transactions of the Royal Society of London Series A*, 370, 2765  
 Altmann M., Roeser S., Demleitner M., Bastian U., Schilbach E., 2017, *A&A*, 600, L4  
 Backman D. E., Paresce F., 1993, in Levy E. H., Lunine J. I., eds, *Protostars and Planets III*. pp 1253–1304

- Balog Z., Muzerolle J., Rieke G. H., Su K. Y. L., Young E. T., Megeath S. T., 2007, *ApJ*, **660**, 1532
- Baraffe I., Homeier D., Allard F., Chabrier G., 2015, *A&A*, **577**, A42
- Barrado y Navascués D., Martín E. L., 2003, *AJ*, **126**, 2997
- Barrado y Navascués D., Stauffer J. R., Jayawardhana R., 2004, *ApJ*, **614**, 386
- Bayo A., Rodrigo C., Barrado Y Navascués D., Solano E., Gutiérrez R., Morales-Calderón M., Allard F., 2008, *A&A*, **492**, 277
- Beccari G., et al., 2010, *ApJ*, **720**, 1108
- Bell C. P. M., Naylor T., Mayne N. J., Jeffries R. D., Littlefair S. P., 2013, *MNRAS*, **434**, 806
- Bell C. P. M., Mamajek E. E., Naylor T., 2015, *MNRAS*, **454**, 593
- Bell C. P. M., Murphy S. J., Mamajek E. E., 2017, *MNRAS*, **468**, 1198
- Binks A. S., Jeffries R. D., 2016, *MNRAS*, **455**, 3345
- Bochanski J. J., West A. A., Hawley S. L., Covey K. R., 2007, *AJ*, **133**, 531
- Boucher A., Lafrenière D., Gagné J., Malo L., Faherty J. K., Doyon R., Chen C. H., 2016, *ApJ*, **832**, 50
- Bouwman J., Lawson W. A., Dominik C., Feigelson E. D., Henning T., Tielens A. G. G. M., Waters L. B. F. M., 2006, *ApJ*, **653**, L57
- Bowler B. P., Liu M. C., Shkolnik E. L., Tamura M., 2015, *ApJS*, **216**, 7
- Bressan A., Marigo P., Girardi L., Salasnich B., Dal Cero C., Rubele S., Nanni A., 2012, *MNRAS*, **427**, 127
- Calvet N., Hartmann L., Strom S. E., 2000, Protostars and Planets IV, p. 377
- Carpenter J. M., Mamajek E. E., Hillenbrand L. A., Meyer M. R., 2006, *ApJ*, **651**, L49
- Carpenter J. M., Mamajek E. E., Hillenbrand L. A., Meyer M. R., 2009, *ApJ*, **705**, 1646
- Chen C. H., Mamajek E. E., Bitner M. A., Pecaut M., Su K. Y. L., Weinberger A. J., 2011, *ApJ*, **738**, 122
- Chen Y., Girardi L., Bressan A., Marigo P., Barbieri M., Kong X., 2014, *MNRAS*, **444**, 2525
- Choi J., Dotter A., Conroy C., Cantiello M., Paxton B., Johnson B. D., 2016, *ApJ*, **823**, 102
- Cody A. M., et al., 2014, *AJ*, **147**, 82
- Costigan G., Scholz A., Stelzer B., Ray T., Vink J. S., Mohanty S., 2012, *MNRAS*, **427**, 1344
- Currie T., et al., 2007a, *ApJ*, **659**, 599
- Currie T., Kenyon S. J., Balog Z., Bragg A., Tokarz S., 2007b, *ApJ*, **669**, L33
- Cutri R. M., Skrutskie M. F., van Dyk S., et al. 2003, 2MASS All Sky Catalog of point sources. Available at <http://www.ipac.caltech.edu/2mass/>
- Cutri R. M., et al., 2014, VizieR Online Data Catalog, **2328**
- D'Alessio P., Calvet N., Hartmann L., Lizano S., Cantó J., 1999, *ApJ*, **527**, 893
- De Marchi G., Panagia N., Guarcello M. G., Bonito R., 2013a, *MNRAS*, **435**, 3058
- De Marchi G., Beccari G., Panagia N., 2013b, *ApJ*, **775**, 68
- Dopita M., Hart J., McGregor P., Oates P., Bloxham G., Jones D., 2007, *Ap&SS*, **310**, 255
- Dotter A., 2016, *ApJS*, **222**, 8
- Dotter A., Chaboyer B., Jevremović D., Kostov V., Baron E., Ferguson J. W., 2008, *ApJS*, **178**, 89
- Elliott P., Bayo A., Melo C. H. F., Torres C. A. O., Sterzik M., Quast G. R., 2014, *A&A*, **568**, A26
- Elliott P., Bayo A., Melo C. H. F., Torres C. A. O., Sterzik M. F., Quast G. R., Montes D., Brahm R., 2016, *A&A*, **590**, A13
- Epchtein N., et al., 1999, *A&A*, **349**, 236
- Espaillet C., Calvet N., D'Alessio P., Hernández J., Qi C., Hartmann L., Furlan E., Watson D. M., 2007, *ApJ*, **670**, L135
- Espaillet C., et al., 2012, *ApJ*, **747**, 103
- Esplin T. L., Luhman K. L., Mamajek E. E., 2014, *ApJ*, **784**, 126
- Fűrész G., Hartmann L. W., Megeath S. T., Szentgyorgyi A. H., Hamden E. T., 2008, *ApJ*, **676**, 1109
- Fang M., van Boekel R., Wang W., Carmona A., Sicilia-Aguilar A., Henning T., 2009, *A&A*, **504**, 461
- Fang M., Kim J. S., van Boekel R., Sicilia-Aguilar A., Henning T., Flaherty K., 2013, *ApJS*, **207**, 5
- Fedele D., van den Ancker M. E., Henning T., Jayawardhana R., Oliveira J. M., 2010, *A&A*, **510**, A72
- Feiden G. A., 2016, *A&A*, **593**, A99
- Gagné J., Lafrenière D., Doyon R., Malo L., Artigau É., 2014, *ApJ*, **783**, 121
- Gagné J., et al., 2015, *ApJS*, **219**, 33
- Gagné J., et al., 2017, *ApJS*, **228**, 18
- Gagné J., et al., 2018, preprint, ([arXiv:1801.09051](https://arxiv.org/abs/1801.09051))
- Gaia Collaboration et al., 2016, *A&A*, **595**, A2
- Gillon M., et al., 2016, *Nature*, **533**, 221
- Girard T. M., van Altena W. F., Zacharias N., et al. 2011, *AJ*, **142**, 15
- Guarcello M. G., et al., 2016, preprint, ([arXiv:1605.01773](https://arxiv.org/abs/1605.01773))
- Haisch Jr. K. E., Lada E. A., Lada C. J., 2001, *ApJ*, **553**, L153
- Hambly N. C., et al., 2001, *MNRAS*, **326**, 1279
- Henning T., Meeus G., 2009, in García P. J. V., ed., Physical Processes in Circumstellar Disks around Young Stars. p. 114 ([arXiv:0911.1010](https://arxiv.org/abs/0911.1010))
- Hernández J., et al., 2007a, *ApJ*, **662**, 1067
- Hernández J., et al., 2007b, *ApJ*, **671**, 1784
- Hillenbrand L. A., 2005, in Livio M., ed., STSci Symposium Series Vol. 19, A Decade of Discovery: Planets Around Other Stars. ([arXiv:astro-ph/0511083](https://arxiv.org/abs/astro-ph/0511083))
- Jayawardhana R., Mohanty S., Basri G., 2003, *ApJ*, **592**, 282
- Johnson J. A., Aller K. M., Howard A. W., Crepp J. R., 2010, *PASP*, **122**, 905
- Johnstone D., Hollenbach D., Bally J., 1998, *ApJ*, **499**, 758
- Kennedy G. M., Kenyon S. J., 2009, *ApJ*, **695**, 1210
- Kraus A. L., Shkolnik E. L., Allers K. N., Liu M. C., 2014, *AJ*, **147**, 146
- Kraus A. L., Cody A. M., Covey K. R., Rizzuto A. C., Mann A. W., Ireland M. J., 2015, *ApJ*, **807**, 3
- Kuchner M. J., et al., 2016, *ApJ*, **830**, 84
- Lada C. J., et al., 2006, *AJ*, **131**, 1574
- Lasker B. M., Lattanzi M. G., McLean B. J., et al. 2008, *AJ*, **136**, 735
- Laughlin G., Bodenheimer P., Adams F. C., 2004, *ApJ*, **612**, L73
- Lawson W. A., Lyo A.-R., Muzerolle J., 2004, *MNRAS*, **351**, L39
- Luhman K. L., Mamajek E. E., 2012, *ApJ*, **758**, 31
- Luhman K. L., et al., 2008, *ApJ*, **675**, 1375
- Mainzer A., et al., 2014, *ApJ*, **792**, 30
- Malo L., Doyon R., Lafrenière D., Artigau É., Gagné J., Baron F., Riedel A., 2013, *ApJ*, **762**, 88
- Malo L., Artigau É., Doyon R., Lafrenière D., Albert L., Gagné J., 2014a, *ApJ*, **788**, 81
- Malo L., Doyon R., Feiden G. A., Albert L., Lafrenière D., Artigau É., Gagné J., Riedel A., 2014b, *ApJ*, **792**, 37
- Mamajek E. E., 2005, *ApJ*, **634**, 1385
- Mamajek E. E., 2009, in Usuda T., Tamura M., Ishii M., eds, American Institute of Physics Conference Series Vol. 1158, American Institute of Physics Conference Series. pp 3–10 ([arXiv:0906.5011](https://arxiv.org/abs/0906.5011)), doi:10.1063/1.3215910
- Mamajek E. E., 2016, in Kastner J. H., Stelzer B., Metchev S. A., eds, IAU Symposium Vol. 314, Young Stars and Planets Near the Sun. p. 21 ([arXiv:1507.06697](https://arxiv.org/abs/1507.06697)), doi:10.1017/S1743921315006250
- Mamajek E. E., Meyer M. R., Liebert J., 2002, *AJ*, **124**, 1670
- Mamajek E. E., et al., 2015b, ArXiv e-prints: 1510.06262,
- Mamajek E. E., et al., 2015a, ArXiv e-prints: 1510.07674,
- McKee C. F., Ostriker E. C., 2007, *ARA&A*, **45**, 565
- Melis C., Zuckerman B., Rhee J. H., Song I., Murphy S. J., Bessell M. S., 2012, *Nature*, **487**, 74
- Mohr P. J., Taylor B. N., 2005, *Rev. Mod. Phys.*, **77**, 1
- Monet D. G., Levine S. E., Canzian B., et al. 2003, *AJ*, **125**, 984
- Moór A., et al., 2011, *ApJ*, **740**, L7
- Moór A., Szabó G. M., Kiss L. L., Kiss C., Ábrahám P., Szulágyi J., Kóspál Á., Szalai T., 2013, *MNRAS*, **435**, 1376
- Morales F. Y., Rieke G. H., Werner M. W., Bryden G., Stapelfeldt K. R., Su K. Y. L., 2011, *ApJ*, **730**, L29
- Morales F. Y., Bryden G., Werner M. W., Stapelfeldt K. R., 2016, *ApJ*, **831**, 97
- Murphy S. J., Lawson W. A., 2015, *MNRAS*, **447**, 1267
- Murphy S. J., Lawson W. A., Bessell M. S., 2010, *MNRAS*, **406**, L50
- Murphy S. J., Lawson W. A., Bessell M. S., 2013, *MNRAS*, **435**, 1325
- Murphy S. J., Lawson W. A., Bento J., 2015, *MNRAS*, **453**, 2220
- Muzerolle J., Hartmann L., Calvet N., 1998, *AJ*, **116**, 455
- Muzerolle J., Calvet N., Briceño C., Hartmann L., Hillenbrand L., 2000, *ApJ*, **535**, L47
- Natta A., Testi L., Muzerolle J., Randich S., Comerón F., Persi P., 2004, *A&A*, **424**, 603
- Nguyen D. C., Jayawardhana R., van Kerkwijk M. H., Brandeker A., Scholz A., Damjanov I., 2009, *ApJ*, **695**, 1648

- Ogihara M., Ida S., 2009, *ApJ*, **699**, 824
- Olczak C., Kaczmarek T., Harfst S., Pflanzner S., Portegies Zwart S., 2012, *ApJ*, **756**, 123
- Pecaut M. J., Mamajek E. E., 2013, *ApJS*, **208**, 9
- Pecaut M. J., Mamajek E. E., 2016, *MNRAS*, **461**, 794
- Pecaut M. J., Mamajek E. E., Bubar E. J., 2012, *ApJ*, **746**, 154
- Pflanzner S., Umbreit S., Henning T., 2005, *ApJ*, **629**, 526
- Raymond S. N., Barnes R., Mandell A. M., 2008, *MNRAS*, **384**, 663
- Reiners A., 2009, *ApJ*, **702**, L119
- Reis W., Corradi W., de Avillez M. A., Santos F. P., 2011, *ApJ*, **734**, 8
- Ribas Á., Bouy H., Merín B., 2015, *A&A*, **576**, A52
- Riddick F. C., Roche P. F., Lucas P. W., 2007, *MNRAS*, **381**, 1067
- Riedel A. R., et al., 2014, *AJ*, **147**, 85
- Robitaille T. P., 2017, *A&A*, **600**, A11
- Röser S., Demleitner M., Schilbach E., 2010, *AJ*, **139**, 2440
- Schlieder J. E., Lépine S., Rice E., Simon M., Fielding D., Tomasino R., 2012, *AJ*, **143**, 114
- Schneider A., Melis C., Song I., 2012, *ApJ*, **754**, 39
- Shkolnik E. L., Anglada-Escudé G., Liu M. C., Bowler B. P., Weinberger A. J., Boss A. P., Reid I. N., Tamura M., 2012, *ApJ*, **758**, 56
- Shu F. H., Adams F. C., Lizano S., 1987, *ARA&A*, **25**, 23
- Sicilia-Aguilar A., Hartmann L. W., Hernández J., Briceño C., Calvet N., 2005, *AJ*, **130**, 188
- Sicilia-Aguilar A., Hartmann L. W., Fürész G., Henning T., Dullemond C., Brandner W., 2006, *AJ*, **132**, 2135
- Siess L., Dufour E., Forestini M., 2000, *A&A*, **358**, 593
- Silverberg S. M., et al., 2016, *ApJ*, **830**, L28
- Slesnick C. L., Carpenter J. M., Hillenbrand L. A., 2006, *AJ*, **131**, 3016
- Spezz L., De Marchi G., Panagia N., Sicilia-Aguilar A., Ercolano B., 2012, *MNRAS*, **421**, 78
- Stauffer J. R., et al., 1999, *ApJ*, **527**, 219
- Teixeira R., Ducourant C., Sartori M. J., Camargo J. I. B., Périé J. P., Lépine J. R. D., Benevides-Soares P., 2000, *A&A*, **361**, 1143
- Thies I., Kroupa P., Goodwin S. P., Stamatellos D., Whitworth A. P., 2010, *ApJ*, **717**, 577
- Tognelli E., Prada Moroni P. G., Degl'Innocenti S., 2011, *A&A*, **533**, A109
- Torres C. A. O., Quast G. R., de La Reza R., da Silva L., Melo C. H. F., 2001, in Jayawardhana R., Greene T., eds, *Astronomical Society of the Pacific Conference Series Vol. 244, Young Stars Near Earth: Progress and Prospects*. p. 43 ([arXiv:astro-ph/0105291](https://arxiv.org/abs/astro-ph/0105291))
- Torres C. A. O., Quast G. R., da Silva L., de La Reza R., Melo C. H. F., Sterzik M., 2006, *A&A*, **460**, 695
- Torres C. A. O., Quast G. R., Melo C. H. F., Sterzik M. F., 2008, *Handbook of Star Forming Regions: Volume II, The Southern Sky*. p. 757
- Viana Almeida P., Santos N. C., Melo C., Ammler-von Eiff M., Torres C. A. O., Quast G. R., Gameiro J. F., Sterzik M., 2009, *A&A*, **501**, 965
- White R. J., Basri G., 2003, *ApJ*, **582**, 1109
- White R. J., Hillenbrand L. A., 2005, *ApJ*, **621**, L65
- Williams J. P., Cieza L. A., 2011, *ARA&A*, **49**, 67
- Wright E. L., Eisenhardt P. R. M., Mainzer A. K., et al. 2010, *AJ*, **140**, 1868
- Wyatt M. C., 2008, *ARA&A*, **46**, 339
- Zuckerman B., Song I., 2004, *ARA&A*, **42**, 685
- Zuckerman B., Song I., 2012, *ApJ*, **758**, 77
- da Silva L., Torres C. A. O., de La Reza R., Quast G. R., Melo C. H. F., Sterzik M. F., 2009, *A&A*, **508**, 833

This paper has been typeset from a  $\text{\TeX}/\text{\LaTeX}$  file prepared by the author.